PERKIN 2 KEYNOTE

Properties of tetramethyleneethane (TME) as revealed by ion chemistry and ion photoelectron spectroscopy

Eileen P. Clifford,[a] Paul G. Wenthold,[b] W. Carl Lineberger,[b] G. Barney Ellison,[a] Cun X. Wang,[c] Joseph J. Grabowski,[c] Fernando Vila[c] and Kenneth D. Jordan[b,c]

[a] *Department of Chemistry & Biochemistry, University of Colorado, Boulder, CO 80309–0215, USA*

[b] *JILA, University of Colorado and National Institute of Standards and Technology, and Department of Chemistry & Biochemistry, University of Colorado, Boulder, CO 80309–0440, USA*

[c] *Department of Chemistry, University of Pittsburgh, Pittsburgh, PA 15260, USA*

The negative ion chemistry and photoelectron spectra of $[CH_2{=}C(CH_3){-}C(CH_2)_2]^-$ and $[(CH_2)_2C{-}C(CH_2)_2]^-$ have been studied. The negative ion photoelectron spectra reveal the tetramethyleneethane diradical, TME, to have two low-lying electronic states, $\tilde{X}$ and $\tilde{a}$. The ground $\tilde{X}$ state is assigned as [TME] ^1A and the excited $\tilde{a}$ state as [TME] $^3B_1$. The energy separation between these states is about 2 kcal mol^{-1}; $\Delta E[\tilde{a}\ ^3B_1 \longleftarrow \tilde{X}\,^1A] \cong 0.1$ eV. The experimental electron affinities of the neutrals are: $E_{ea}[CH_2{=}C(CH_3){-}C(CH_2)_2] = 0.654 \pm 0.010$ eV and $E_{ea}[(CH_2)_2C{-}C(CH_2)_2] = 0.855 \pm 0.010$ eV. The experimental gas phase acidities are: $\Delta_{acid}H_{298}[CH_2{=}C(CH_3){-}C(CH_2)CH_2{-}H] = 388 \pm 3$ kcal mol^{-1} and $\Delta_{acid}H_{298}[(CH_2)_2C{-}C(CH_2){-}CH_2{-}H] = 388 \pm 4$ kcal mol^{-1}. These findings can be used to establish the bond energies and heats of formation: $DH_{298}[CH_2{=}C(CH_3){-}C(CH_2)CH_2{-}H] = 90 \pm 3$ kcal mol^{-1} and $\Delta_f H_{298}[(CH_2)_2C{-}C(CH_3){=}CH_2] = 48 \pm 3$ kcal mol^{-1}; $DH_{298}[(CH_2)_2C{-}C(CH_2)CH_2{-}H] = 94 \pm 4$ kcal mol^{-1} and $\Delta_f H_{298}[(CH_2)_2C{-}C(CH_2)_2] = 90 \pm 5$ kcal mol^{-1}.

Introduction

In 1970 Paul Dowd reported[1] the preparation of the tetramethyleneethane diradical (TME) and described the EPR spectrum of this hydrocarbon. For nearly 30 years TME and its derivatives have fascinated organic chemists and have been scrutinized by many.[2] We have undertaken a study of the properties of two negative ions derived from 2,3-dimethylbuta-1,3-diene, $CH_2{=}C(CH_3){-}C(CH_3){=}CH_2$: the 2-(isopropenyl)allyl

(1)

$[CH_2{=}C(CH_3){-}C(CH_2)_2]^-$, *m*/*z* 81 $[(CH_2)_2C{-}C(CH_2)_2]^-$, *m*/*z* 80

anion *m*/*z* 81 and the tetramethyleneethane anion, *m*/*z* 80. These ions provide novel gateways[3] to the spectroscopic and thermodynamic properties of the disjoint diradical TME, and the related allylic radical, 2-(isopropenyl)allyl.

(2)

2-(Isopropenyl)allyl radical TME diradical

The gas phase chemistry and photoelectron spectroscopy of these negative ions provide: (*a*) the electron affinities of the 2-(isopropenyl) allyl radical, $E_{ea}[CH_2{=}C(CH_3){-}C(CH_2)_2]$, and the TME diradical, $E_{ea}[(CH_2)_2C{-}C(CH_2)_2]$, (*b*) information on the lowest ^{1}TME and ^{3}TME states, and (*c*) the gas phase acidities of the parent neutrals $\Delta_{acid}G_{298}[CH_2{=}C(CH_3){-}C(CH_2){-}CH_2{-}H]$ and $\Delta_{acid}G_{298}[(CH_2)_2C{-}C(CH_2)CH_2{-}H]$.

TME is the prototype of an unusual family of reactive intermediates termed disjoint diradicals.[2,4] These species have a pair of low-lying electronic states, one singlet and the other triplet, which are nearly degenerate. The extreme reactivity of TME diradicals prevents the production of high concentrations of these species and, consequently, their physical characterization has been difficult. The pioneering studies[1] of TME employed magnetic resonance techniques to examine small samples of diradicals isolated in a cryogenic matrix. EPR spectroscopy can monitor signals[5,6] from about 10^8 spins. This technique only responds to paramagnetic species and is insensitive to the huge excess of the diamagnetic precursor used to produce the target diradicals. For about 25 years, EPR has been the principle analytical tool for characterizing disjoint diradicals.[7–12] One of the most recent exciting developments in this area is the application of mass spectrometric[13,14] and laser techniques[15–18] to the study of diradicals. The reaction dynamics of diradicals are beginning to be scrutinized by theoretical methods.[19,20]

Many *ab initio* electronic structure calculations have been reported for TME and TME derivatives.[21–28] However, obtaining a definitive order of the singlet and triplet states of these species is not easy because of their 'near' degeneracy. The consensus is that for the TME diradical itself the lowest two states, ^{1}[TME] and ^{3}[TME], lie within 3 kcal mol^{-1} of each other but the ordering is a topic of considerable debate. The EPR spectrum of TME is clearly that of a triplet and it is indefinitely stable; a linear Curie plot suggests that TME is a ground state triplet. It was recently reported[29] that the lowest singlet and triplet states of the TME derivative, 2,3-dimethylenecyclohexane-1,4-diyl, are degenerate.

Negative ion chemistry and spectroscopy affords a new avenue to study the properties of diradicals in general and TME in particular. It has been clearly demonstrated that O^- chemistry[30] offers a rational synthesis for the $[TME]^-$ ion, *m*/*z* 80 in (1). Reaction of $CH_2{=}C(CH_3){-}C(CD_3){=}CD_2$ with O^- generated only the *m*/*z* 84 $[TME]^-$ ion; eqn. (3). The absence of the *m*/*z* 83

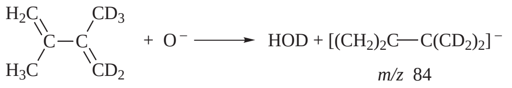

(3)

Table 1 (*a*) Proton transfer studies of 2,3-dimethylbuta-1,3-diene: $CH_2{=}C(CH_3){-}C(CH_3){=}CH_2$

$$[CH_2{=}C(CH_3){-}C(CH_2)_2]^- + HA \underset{k_{-5}}{\overset{k_5}{\rightleftharpoons}} CH_2{=}C(CH_3){-}C(CH_3){=}CH_2 + A^-$$

AH	$\Delta_{acid}G_{298}$/kcal mol^{-1}	$\Delta_{acid}H_{298}$/kcal mol^{-1}	k_5	k_{-5}
D_2O	386.1 ± 0.2	392.0 ± 0.1	No[a]	Yes
H_2O	384.1 ± 0.2	390.7 ± 0.1	No	Yes
Furan	382.9 ± 0.2	390.7 ± 0.2	No	Trace
CH_3OD	376.9 ± 0.7	383.5 ± 0.7	Yes	No
CH_3OH	375.0 ± 0.7	381.6 ± 0.7	Yes	No
$CH_3CH_2CH(OH)CH_3$	367.6 ± 2.0	374.2 ± 2.1	Yes	No
CH_3CN	365.2 ± 2.0	372.9 ± 2.1	Yes	No

(*b*) Proton transfer studies of 2-(isopropenyl)allyl radical: $CH_2{=}C(CH_3){-}C(CH_2)_2$

$$[(CH_2)_2C{-}C(CH_2)_2]^- + HA \underset{K_{-6}}{\overset{k_6}{\rightleftharpoons}} CH_2{=}C(CH_3){-}C(CH_2)_2 + A^-$$

AH	$\Delta_{acid}G_{298}$/kcal mol^{-1}	$\Delta_{acid}H_{298}$/kcal mol^{-1}	k_6	k_{-6}
D_2O	386.1 ± 0.2	392.0 ± 0.1	No[a]	—
H_2O	384.1 ± 0.2	390.7 ± 0.1	No	—
Furan	382.9 ± 0.2	390.7 ± 0.2	Trace	—
$CH_2{=}C(CH_3){-}C(CH_3){=}CH_2$	380 ± 3	388 ± 3	No	—
CH_3OD	376.9 ±	383.5 ± 0.7	Yes	—
CH_3OH	375.1 ± 0.7	381.6 ± 0.4	Yes[b]	—
$CH_3CH_2CH(OH)CH_3$	367.6 ± 2.0	374.2 ± 2.1	Yes	—
CH_3CN	365.2 ± 2.0	372.9 ± 2.1	Yes	—

[a] H/D isotope exchange observed. [b] Proton transfer between methanol and $[TME]^-$ is 16% efficient; $k(CH_3OH + [TME]^-)$ is 3.0×10^{-10} cm^3 s^{-1}.

or 85 carbanions as products from (3) excludes carbene anion structures as products of O^- reaction; the only product in (3) is $[TME]^-$. In addition to establishing a structure for the $[TME]^-$ *m*/*z* 80 ion, this initial study[3] placed an approximate bound on the enthalpy of deprotonation of the allylic radical: $\Delta_{acid}H_{298}[(CH_2)_2C{-}C(CH_2)CH_2{-}H] = 385.7 \pm 5$ kcal mol^{-1}.

In this paper we explore the ion chemistry and photoelectron spectroscopy of the 2-(isopropenyl)allyl radical anion, $[CH_2{=}C(CH_3){-}C(CH_2)_2]^-$ (*m*/*z* 81) and that of the TME anion, $[(CH_2)_2C{-}C(CH_2)_2]^-$ (*m*/*z* 80). Our experiments establish more precise values of the enthalpies of deprotonation, $\Delta_{acid}H_{298}$-$[CH_2{=}C(CH_3)C(CH_2)CH_2{-}H]$ and $\Delta_{acid}H_{298}[(CH_2)_2CC(CH_2)$-$CH_2{-}H]$, as well as the electron affinities, $E_{ea}[CH_2{=}C(CH_3){-}C(CH_2)_2]$ and $E_{ea}[(CH_2)_2C{-}C(CH_2)_2]$. These measurements are combined to provide the bond energies and the absolute heats of formation of the 2-(isopropenyl)allyl radical and for TME itself. For TME, we assign the ground $\tilde{X}$ state as ^1A and the excited $\tilde{a}$ state as $^3B_1$; the splitting between them is about 2 kcal mol^{-1}.

Experimental

A. Negative ion photoelectron spectroscopy

The photoelectron spectra were collected on a spectrometer that has been described elsewhere.[15,31] We have used O^- chemistry (*vide supra*) and 2,3-dimethylbuta-1,3-diene to generate ion beams of *m*/*z* 80 and 81. The two ions at *m*/*z* 80 and 81 were separated by a Wien velocity filter and photodetached by a CW Ar III ion laser that produces 50–100 W of 351.1 nm light in the circulating build-up cavity. The photodetached electrons are focused and passed through a hemispherical energy analyzer, with an instrumental resolution (FWHM) of 6–10 meV. In order to reduce rotational broadening in the photodetachment spectra, we bathe part of the flow tube with liquid N_2. The vibrational and rotational temperatures of the ions are roughly 200 K.

The photoelectron spectra are calibrated[32] with respect to O^- and transformed into the center-of-mass (cm) frame by a standard[33] expression where E is the cm kinetic energy (eV) of an electron detached from an ion of mass M (amu) that is passed by the energy analyzer when the slit voltage is V. The beam energy is W, m_e is the mass of an electron, M is the mass of the target ion, M_{cal} is the mass of the calibration ion observed at V_{cal}, and γ is the dimensionless scale compression factor (typically 1.000 ± 0.006).

$$E = E_{cal} + \gamma(V - V_{cal}) + m_eW\left(\frac{1}{M_{cal}} - \frac{1}{M}\right) \qquad (4)$$

B. Flowing afterglow

A flowing afterglow[34–36] was employed to bracket the gas phase basicities of the 2-(isopropenyl)allyl radical anion, $[CH_2{=}C(CH_3){-}C(CH_2)_2]^-$ (*m*/*z* 81) and of the TME anion, $[(CH_2)_2C{-}C(CH_2)_2]^-$ (*m*/*z* 80). The O^- ion was generated in the source by electron ionization of traces of nitrous oxide in the helium buffer gas (0.3 Torr). The bracketing acids, Table 1, were introduced through a manifold of inlets and the reactant and product ions were monitored with a detection quadrupole mass filter coupled with an electron multiplier. When required, the flow rates of the neutral reagents were measured by monitoring the pressure increase with time in a calibrated volume system.

Results

A. The acidity of 2,3-dimethylbuta-1,3-diene and 2-(isopropenyl)-allyl radical

To bracket the acidities, the conjugate bases of 2,3-dimethylbuta-1,3-diene and the 2-(isopropenyl)allyl radical, $[CH_2{=}C(CH_3){-}C(CH_2)_2]^-$ and $[(CH_2)_2C{-}C(CH_2)_2]^-$, were combined with of a set[37–40] of standard acids (HA) and it was observed whether proton transfer occurred (+) or not (−) and the conjugate base was produced, A^-.

The gas-phase acidity of 2,3-dimethylbuta-1,3-diene was determined both by reaction of its conjugate base with acids of known acidity and by reaction of the diene with well characterized bases (k_5 and k_{-5} in Table 1), eqn. (5).

$$[CH_2{=}C(CH_3){-}C(CH_2)_2]^- + HA \rightleftharpoons CH_2{=}C(CH_3){-}C(CH_3){=}CH_2 + A^- \qquad (5)$$

For each forward and reverse reaction, the occurrence of a proton transfer is noted in Table 1. Based on the results summarized in Table 1, we conclude that the acidity of 2,3-

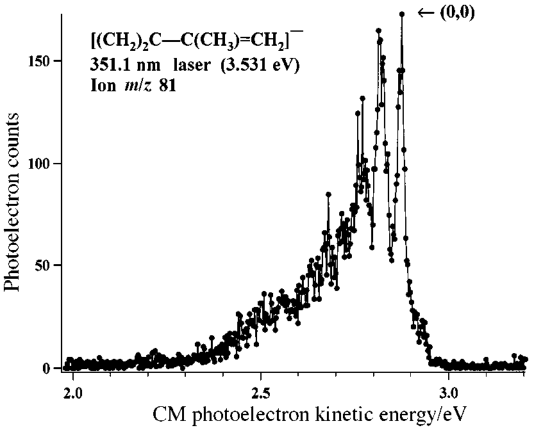

Fig. 1 A plot of the negative ion spectrum of the [CH_2=C(CH_3)–C(CH_2)$_2$]$^-$ ion, *m*/*z* 81; detachment laser λ_0 = 351.1 nm (3.531 eV)

dimethylbuta-1,3-diene is between that of furan and CH_3OD or $\Delta_{acid}G_{298}$[CH_2=C(CH_3)C(CH_2)CH_2–H] = 380 ± 3 kcal mol^{-1}. Several points about eqn. (5) deserve further elaboration. For the forward reaction with HA = D_2O, no proton transfer was observed, but facile H/D exchange is detected; the lack of proton transfer but facile exchange is consistent with the relative acidity of the two acids involved. Secondly, the lack of proton transfer from furan and the slow abstraction by furanide is consistent with an acid–base reaction with little driving force and involving a delocalized base.

Included in Table 1 are the results for the bracketing experiments conducted to determine the acidity of the 2-(isopropenyl)-allyl radical, CH_2=C(CH_3)–C(CH_2)$_2$, eqn. (6). In eqn. (6) the

$$[(CH_2)_2C–C(CH_2)_2]^- + HA \rightleftharpoons CH_2{=}C(CH_3)–C(CH_2)_2 + A^- \quad (6)$$

neutral radical is not an available reagent and hence the bracketing studies can only be determined in one direction. Based on the results summarized in Table 1, we conclude that $\Delta_{acid}G_{298}$[(CH_2)$_2$C–C(CH_2)CH_2–H] = 381 ± 4 kcal mol^{-1}. The 1 kcal mol^{-1} decrease in acidity of the radical as compared with its parent is primarily based on the differences of k_5 and k_6 for furan as a neutral. The larger error bar on the radical acidity reflects additional uncertainty due to the fact that bracketing was determined from one direction only.

We use standard expressions[41] to estimate the entropy and to compute values for the enthalpy of deprotonation from the gas phase acidity: $\Delta_{acid}G_{298}[AH] = \Delta_{acid}H_{298}[AH] - T\Delta_{acid}S_{298}[AH]$. For the case of dimethylbutadiene we adopt $\sigma(C_{2h})$ for the parent and $\sigma(C_s)$ for the allylic anion to compute $\Delta_{acid}S_{298}$ = 27.3 cal mol^{-1} K^{-1}; consequently we find $\Delta_{acid}H_{298}$[CH_2=C(CH_3)–C(CH_2)CH_2–H] = 388 ± 3 kcal mol^{-1}. With the 2-(isopropenyl)-allyl radical we use $\sigma(C_s)$ for the parent and $\sigma(D_{2d})$ for the TME$^-$ anion and recover $\Delta_{acid}S_{298}$ = 24.6 cal mol^{-1} K^{-1}. Consequently we arrive at the enthalpy for deprotonation of the 2-(isopropenyl)allyl radical: $\Delta_{acid}H_{298}$[(CH_2)$_2$C–C(CH_2)CH_2–H] = 388 ± 4 kcal mol^{-1}.

B. Photoelectron spectroscopy

Fig. 1 presents the photoelectron spectrum of the [CH_2=C(CH_3)–C(CH_2)$_2$]$^-$ ion, *m*/*z* 81. The origin of the spectrum is marked by (0,0) at 2.877 ± 0.010 eV and corresponds to an electron affinity for the 2-(isopropenyl)allyl radical of E_{ea}[CH_2=C(CH_3)–C(CH_2)$_2$] = 0.654 ± 0.010 eV or 15.1 ± 0.2 kcal mol^{-1}. The active mode in the 2-(isopropenyl)allyl radical anion photodetachment spectrum at 440 cm^{-1} is attributed to the 'allylic C–C–C scissors' mode.

Earlier[42] the photoelectron spectrum of the analogous 2-methylallylic anion was studied and it was reported that E_{ea}[CH_2C(CH_3)CH_2] = 0.505 ± 0.006 eV. The active mode (428

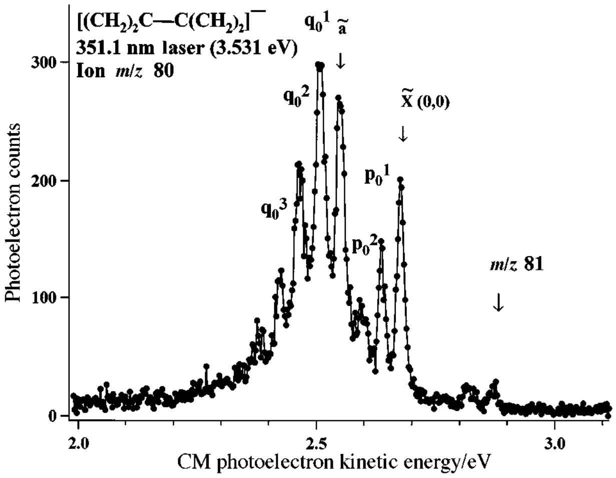

Fig. 2 A plot of the negative ion spectrum of the [(CH_2)$_2$C–C(CH_2)$_2$]$^-$ ion, *m*/*z* 80; detachment laser λ_0 = 351.1 nm (3.531 eV). Because of imperfect mass-resolution this spectrum is slightly contaminated with peaks due to the [CH_2=C(CH_3)–C(CH_2)$_2$]$^-$ ion at *m*/*z* 81.

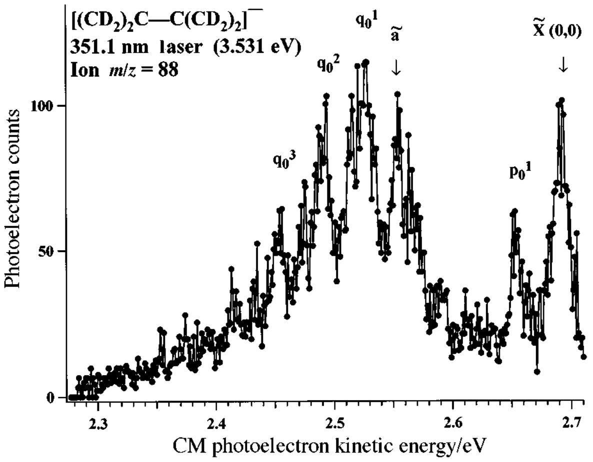

Fig. 3 A plot of the negative ion spectrum of the [(CD_2)$_2$C–C(CD_2)$_2$]$^-$ ion, *m*/*z* 88; detachment laser λ_0 = 351.1 nm (3.531 eV)

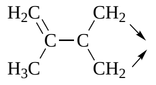

(7)

cm^{-1}) in the CH_2C(CH_3)CH_2 spectrum was observed to be harmonic and was assigned to ν_1, the CCC scissors mode.

Fig. 2 presents the photoelectron spectrum of the [TME]$^-$ anion, [(CH_2)$_2$C–C(CH_2)$_2$]$^-$, *m*/*z* 80. The spectrum clearly shows detachment to two different electronic states of the TME diradical, [(CH_2)$_2$C–C(CH_2)$_2$]. The ground state of TME is labeled $\tilde{X}$ and the origin of the transition is at (0,0) = 2.676 ± 0.010 eV, corresponding to an E_{ea}[(CH_2)$_2$C–C(CH_2)$_2$] = 0.855 ± 0.010 eV or 19.7 ± 0.2 kcal mol^{-1}. The active mode excited in the $\tilde{X}$ state is called ν_p at 335 cm^{-1}. The second TME electronic state is labeled ã and has an apparent origin at 2.548 ± 0.010 eV and an active vibrational mode: ν_q = 335 cm^{-1}. The apparent splitting between the two lowest electronic states of the [(CH_2)$_2$C–C(CH_2)$_2$] diradical is $\Delta E[\tilde{a} \longleftarrow \tilde{X}]$ = 0.13 ± 0.01 eV or 3.0 ± 0.3 kcal mol^{-1}.

We have also prepared beams of the ([$^2H_8$]TME)$^-$ ions from the reaction of O$^-$ with CD_2=C(CD_3)–C(CD_3)=CD_2, and the photoelectron spectrum of the resulting [(CD_2)$_2$C–C(CD_2)$_2$]$^-$ ion is displayed in Fig. 3. For this isotopomer, we observe the $\tilde{X}$ state at (0,0) = 2.689 ± 0.010 eV, and E_{ea}[(CD_2)$_2$C–C(CD_2)$_2$] = 0.842 ± 0.010 eV or 19.4 ± 0.2 kcal mol^{-1}. The $\tilde{X}$ ground state of [(CD_2)$_2$C–C(CD_2)$_2$] displays vibrational structure due to ν_p at 260 ± 10 cm^{-1}. The origin of the ã state of [(CD_2)$_2$C–

Table 2 Energetics of 2-(isopropenyl)allyl radical and TME diradical

		Reference
(*a*) 2-(Isopropenyl)allyl radical, $CH_2{=}C(CH_3){-}C(CH_2)_2$		
$E_{ea}(\tilde{X}^2A''\ [CH_2{=}C(CH_3){-}C(CH_2)_2])$/eV	0.654 ± 0.010 (15.1 ± 0.2 kcal mol^{-1})	This work
$\Delta_{acid}H_{298}[CH_2{=}C(CH_3){-}C(CH_2)CH_2{-}H]$/kcal mol^{-1}	388 ± 3	This work
$DH_{298}[CH_2{=}C(CH_3){-}C(CH_2)CH_2{-}H]$/kcal mol^{-1}	90 ± 3	This work
$D_0[CH_2{=}C(CH_3){-}C(CH_2)CH_2{-}H]$/kcal mol^{-1}	88 ± 3	This work
$\Delta_fH_{298}[CH_2{=}C(CH_3){-}C(CH_3){=}CH_2]$/kcal mol^{-1}	10.8 ± 0.3	45
$\Delta_fH_{298}[(CH_2)_2C{-}C(CH_3){=}CH_2]$/kcal mol^{-1}	48 ± 3	This work
(*b*) TME diradical, $(CH_2)_2C{-}C(CH_2)_2$		
$E_{ea}(\tilde{X}\ ^1A\ [(CH_2)_2C{-}C(CH_2)_2])$/eV	0.855 ± 0.010 (19.7 ± 0.2 kcal mol^{-1})	This work
$\Delta_{acid}H_{298}[(CH_2)_2C{-}C(CH_2)CH_2{-}H]$/kcal mol^{-1}	388 ± 4	This work
$DH_{298}[(CH_2)_2C{-}C(CH_2)CH_2{-}H]$/kcal mol^{-1}	94 ± 4	This work
$D_0[(CH_2)_2C{-}C(CH_2)CH_2{-}H]$/kcal mol^{-1}	93 ± 4	This work
$\Delta_fH_{298}[(CH_2)_2C{-}C(CH_2)_2]$/kcal mol^{-1}	90 ± 5	This work
$\Delta E[\text{TME}\ \tilde{a}\ ^3B_1 \leftarrow \text{TME}\ \tilde{X}^1A]$/kcal mol^{-1}	2	This work

$C(CD_2)_2]$ is assigned as 2.557 ± 0.010 eV with an active mode, ν_q at 267 cm^{-1}; consequently the apparent $\Delta E(\tilde{a} \longleftarrow \tilde{X}, [^2H_8]\text{TME})$ splitting is 0.13 ± 0.01 eV or 3.0 ± 0.3 kcal mol^{-1} and is identical with the $[^2H_0]$TME isomer.

In addition to the low-lying $\tilde{X}$ and $\tilde{a}$ states, we observe weak transitions to a third state of TME which we call $\tilde{Z}$, with $\Delta E[\tilde{Z} \longleftarrow \tilde{X}] = 1.93 \pm 0.01$ eV or 44.6 ± 0.3 kcal mol^{-1}; this band will appear in the visible range of the electromagnetic spectrum of TME at about 645 nm.

C. Experimental thermochemistry of the 2-(isopropenyl)allyl radical and TME

If one can measure the enthalpy of deprotonation for a species AH $[\Delta_{acid}H_{298}(AH)]$ and separately find the electron affinity of the corresponding radical $[E_{ea}(A)]$, then a simple cycle using the ionization potential (E_i) of H provides the bond enthalpy $[DH_{298}(AH)]$; eqn. (8).

$$\Delta_{acid}H_{298}(AH) = DH_{298}(AH) + E_i(H) - E_{ea}(A) - \int_0^{298} dT\,[C_p(A) - C_p(A^-) + C_p(H) - C_p(H^+)] \quad (8)$$

Since the sum of the integrated heat capacities is always[43] small (≤0.3 kcal mol^{-1}), the term in brackets can be ignored and we employ a more common expression,[44] $\Delta_{acid}H_{298}(AH) \cong DH_{298}(AH) + E_i(H) - E_{ea}(A)$. Use of the measured electron affinities and hydrocarbon acidities leads to the experimental bond enthalpies (Table 2), $DH_{298}[CH_2{=}C(CH_3){-}C(CH_2)CH_2{-}H] = 90 \pm 3$ kcal mol^{-1} and $DH_{298}[(CH_2)_2C{-}C(CH_2)CH_2{-}H] = 94 \pm 4$ kcal mol^{-1}. The bond enthalpy at 298 K and the bond energy at 0 K are related by the heat capacities; eqn. (9).

$$DH_{298}(RH) = D_0(RH) + \int_0^{298} dT\,[C_p(R) + C_p(H) - C_p(RH)] \cong D_0(RH) + \int_0^{298} dT\,[C_p(H)] \quad (9)$$

Since the integrated heat capacity for H atom is just 5/2 *RT*, we compute $D_0[CH_2{=}C(CH_3)C(CH_2)CH_2{-}H] = 88 \pm 3$ kcal mol^{-1} and $D_0[(CH_2)_2CC(CH_2)CH_2{-}H] = 93 \pm 4$ kcal mol^{-1}. The heat of formation of dimethylbutadiene is established[45] as $\Delta_fH_{298}[CH_2{=}C(CH_3){-}C(CH_3){=}CH_2] = 10.78 \pm 0.26$ kcal mol^{-1}; consequently the bond enthalpies imply $\Delta_fH_{298}[(CH_2)_2C{-}C(CH_3){=}CH_2] = 48 \pm 3$ kcal mol^{-1} and $\Delta_fH_{298}[(CH_2)_2C{-}C(CH_2)_2] = 90 \pm 5$ kcal mol^{-1}.

Discussion

The photoelectron spectra in Figs. 2 and 3 demonstrate that the TME diradical has two electronic states that are within 3 kcal mol^{-1} of each other. The spectra are remarkably simple and suggest there are only small differences between the molecular structures of the $[\text{TME}]^-$ anion and the two low-lying states of the TME diradical. The detachment process, $\text{TME} \longleftarrow [\text{TME}]^-$, excites only a single, low frequency (335 cm^{-1}) mode in both $\tilde{X}$ and $\tilde{a}$ states of the product diradical. Other than the earlier EPR studies, there have been no spectroscopic measurements of the $(CH_2)_2C{-}C(CH_2)_2$ diradical. In particular, there are no matrix vibrational studies to which we can appeal to assign the 335 cm^{-1} active mode.

Because TME might be described as a 'doubly allylic diradical,' important clues to the understanding of the vibrational structure in the photoelectron spectrum of $[(CH_2)_2C{-}C(CH_2)_2]^-$ are likely to be gleaned from the photoelectron spectrum[42,46,47] of allyl anion, $[CH_2CHCH_2]^-$. The electron affinity of the allyl radical is $E_{ea}[CH_2CHCH_2] = 0.481 \pm 0.008$ eV and upon deuteriation this value shifts to $E_{ea}[CD_2CDCD_2] = 0.464 \pm 0.006$ eV. Methylation of the allylic ion produces a shift[42] in the electron affinity; $E_{ea}[CH_2C(CH_3)CH_2] = 0.505 \pm 0.006$ eV. The photoelectron spectrum of $[(CH_2)_2C{-}C(CH_2)_2]^-$ is consistent with the simpler allylic systems; the E_{ea}(TME) red shifts by 13 meV upon deuteriation, $[(CH_2)_2C{-}C(CH_2)_2] \longrightarrow [(CD_2)_2C{-}C(CD_2)_2]$, which compares with the 17 meV allyl shift, $C_3H_5 \longrightarrow C_3D_5$. Detachment[42] of an electron from $[CH_2CHCH_2]^-$ excites the C–C–C scissors mode of the CH_2CHCH_2 radical, ν_7, at 425 cm^{-1} that shifts to 345 cm^{-1} in C_3D_5. CH_2CHCH_2 has a C_{2v} structure with a C–C bond length of 1.428 ± 0.013 Å and a C–C–C angle of 124.6° ± 3.4°. In contrast, $[CH_2CHCH_2]^-$ has a more open structure with a C–C bond length of 1.45 ± 0.02 Å and a C–C–C angle of 132 ± 5°.

The photoelectron spectrum of the $[(CH_2)_2C{-}C(CH_2)_2]^-$ ion resembles that of $[CH_2CHCH_2]^-$ even though the E_{ea} of TME, 0.855 ± 0.010 eV, is roughly twice that of allyl, 0.481 ± 0.008 eV. By analogy with allyl, we assign both the TME active modes, $\tilde{X}\ \nu_p$ and $\tilde{a}\ \nu_q$ at 335 cm^{-1}, to be excitation of the symmetric $CH_2{-}C{-}CH_2$ bend. The active mode in CH_2CHCH_2 is ν_7 and it falls 80 cm^{-1} upon deuteriation. From Figs. 2 and 3, the ν_p active mode in $\tilde{X}\ [(CH_2)_2C{-}C(CH_2)_2]$ shifts 75 cm^{-1} upon deuteriation while $\nu_q\ \tilde{a}\ [(CH_2)_2C{-}C(CH_2)_2]$ drops by about 68 cm^{-1} in $\tilde{a}\ [(CD_2)_2C{-}C(CD_2)_2]$. Based on these analogies and the results of B3LYP/6–31+G(d) electronic structure calculations, we assign the active modes, ν_p in $\tilde{X}$ TME and ν_q in $\tilde{a}$ TME, to the symmetric bending mode.

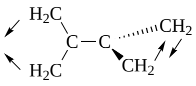

(10)

How can we assign the two low-lying electronic states in the photoelectron spectrum of TME in Figs. 2 and 3? Direct

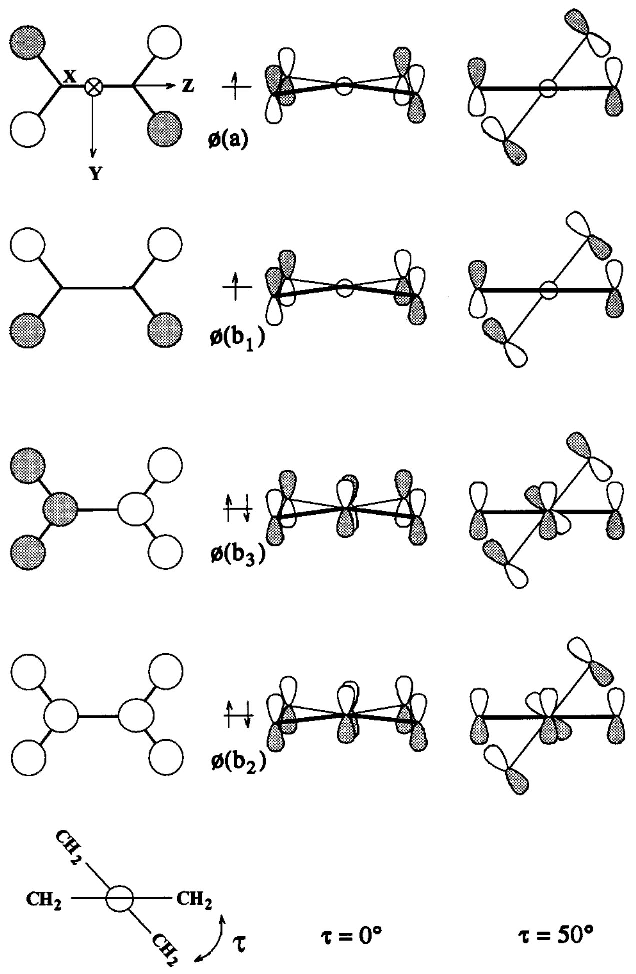

Fig. 4 Sketches of the a, b_1, b_2, and b_3 π orbitals of TME

detachment of $[TME]^-$ to generate a free electron should produce the triplet-coupled TME diradical with a probability three times greater than that of the singlet state of the TME diradical.[48] A triplet : singlet intensity ratio of 3 : 1 has been observed for several diradical/carbene species, including methylene,[15] *o*-benzyne,[16] trimethylenemethane,[49] and diazocarbene.[50] The ratio of the integrated areas of the $\tilde{X}$ and $\tilde{a}$ states in Fig. 2 is measured to be $[\tilde{a}/\tilde{X}] = [3.2/1]$. This finding leads us to assign the $\tilde{X}$ state as $^1[(CH_2)_2C–C(CH_2)_2]$ and the $\tilde{a}$ state as $^3[(CH_2)_2C–C(CH_2)_2]$. The difference in the ^{1}TME and ^{3}TME Franck–Condon envelopes is also consistent with this assignment. Since the geometries of ^{1}TME and TME^- are both D_{2d} (*vide infra*) we anticipate a set of nearly vertical Franck–Condon factors; a more open set of Franck–Condon factors is compatible with the $^3TME\ (D_2) \longleftarrow TME^-(D_{2h})$ assignment.

To provide further support for the above assignments, we have carried out electronic structure calculations on the low-lying electronic states of TME and $[TME]^-$. Because it is known from earlier theoretical studies that the lowest lying singlet and triplet states of TME are twisted,[21,22,27] we find it useful to discuss the various states within the context of D_2 symmetry; see Fig. 4. The two nearly degenerate orbitals that are responsible for the diradical character of TME are then of a and b_1 symmetry. Fig. 5 shows the variation of the energies of the orbitals, $\{\phi_{b_1}, \phi_a\}$ with the torsional angle, τ. The two frontier orbitals are non-degenerate at both the planar and perpendicular structures, but they cross in energy at an intermediate value of the dihedral angle ($\cong$ 40°). This is because the b_1 orbital is bonding between the two allyl groups for small values of the dihedral angle, but is antibonding for large dihedral angles. Precisely the opposite situation exists for the a orbital.

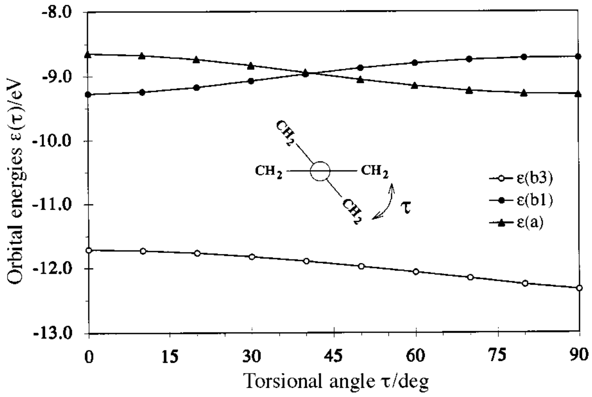

Fig. 5 Variation in energy of the $\phi(a)$ and $\phi(b_1)$ frontier orbitals of TME with respect to the dihedral angle, τ. The orbital energies are from UHF/6–31+G(d) calculations on TME $^3B_1$.

If we suppress the contributions of the inner electrons for simplicity, the wavefunctions for the lowest singlet and triplet states of TME are those given in eqns. (11a) and (11b).

$$^1TME\ (^1A) = c_1\, \phi_a^{\,2} - c_2\phi_{b_1}^{\,2} \qquad (11a)$$

$$^3TME\ (^3B_1) = \phi_a\phi_{b_1} - \phi_{b_1}\phi_a \qquad (11b)$$

The minimum energy structure for the triplet state is expected to occur at a dihedral angle close to that at which the two orbitals cross, an expectation borne out by electronic structure calculations. The calculations presented below give an equilibrium ^{3}TME equilibrium structure with $\tau \cong 50°$. If the singlet state had equal weights on the two configurations, it would also be expected to be twisted to about the same extent as the triplet. However, the two-configurational SCF (TCSCF) as well as higher level calculations[27] reveal that the singlet has a perpendicular (D_{2d}) structure, consistent with the greater occupation of the $\phi_a^{\,2}$ configuration. (The TCSCF calculations give $c_1 = 0.79$, $c_2 = -0.61$).

The TME anion has two low-lying states: $[TME]^-\ (^2B_1) = \phi_a^{\,2}\phi_{b_1}$ and $[TME]^-\ (^2A) = \phi_a\phi_{b_1}^{\,2}$. One expects that the $^2B_1$ $[TME]^-$ anion should have a D_{2d} equilibrium structure and the higher-lying ^2A anion should be either planar or only slighted twisted away from planar. To confirm these predictions and to aid in interpreting the spectra, we have optimized the geometries and calculated the harmonic vibrational frequencies of the two anion states and of the $^3B_1$ of neutral TME using the B3LYP method[51] and the 6–31+G(d) basis set.[52,53] In addition, we have carried out two-configurational SCF (TCSCF) calculations on the lowest singlet and triplet states. (In the case of the triplet, this is equivalent to a ROHF calculation.) The frequency calculations made use of analytical second derivatives. All calculations were carried out using the GAUSSIAN 94 suite of computer programs.[54]

The calculations confirm the qualitative picture presented above: namely, the lower energy anion is predicted to be $^2B_1$, with a D_{2d} structure, with the ^2A anion predicted to lie about 3.5 kcal mol^{-1} higher in energy and to be twisted only slightly from planarity. The B3LYP calculations place the $^2B_1$ anion 0.92 eV below the $^3B_1$ state of neutral TME, in very good agreement with the present experimental result (0.99 ± 0.01 eV).

We now consider the implications of the calculations for the vibrational structure seen in the photoelectron spectrum of $[TME]^-$. Given the sizable energy gap between the two anion states, little population of the less stable ^2A anion is expected under experimental conditions. In that case, the photoelectron spectrum can be interpreted as arising from the TME $\tilde{a}\ ^3B_1 \longleftarrow [TME]^-\ \tilde{X}\ ^2B_1$ and TME $\tilde{X}\ ^1A \longleftarrow [TME]^-\ \tilde{X}\ ^2B_1$ transitions. In addition to the differences in the dihedral angles discussed above, the calculations predict appreciably different allylic CCC angles for the different states. In particular, the

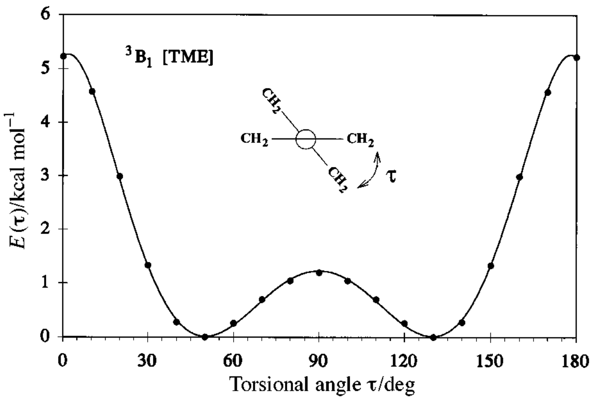

Fig. 6 Twisting potential energy curve [B3LYP/6–31+G(d)] of TME $^3B_1$ with all geometrical parameters (except the dihedral angle, τ) held fixed at the equilibrium structure

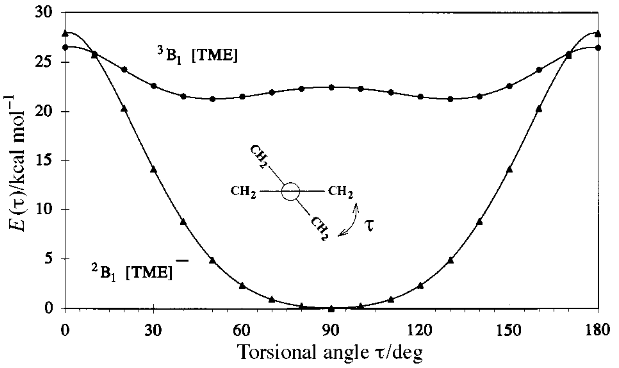

Fig. 7 Twisting potential energy curves [B3LYP/6–31+G(d)] of TME $^3B_1$ and TME$^-$ $^2B_1$ with all geometrical parameters (except the dihedral angle, τ) held fixed at the equilibrium structure

CCC angle is predicted to be 128.4° in the $^2B_1$ anion but only 121.9° in $^3B_1$ TME. This difference is close to that mentioned above for going from the anion to the neutral of the allyl radical. Moreover, the TCSCF/ROHF calculations predict the CCC angle to be about 1.5° larger in the singlet than in the triplet state.

These results lead one to expect significant excitation of the allylic CCC scissors mode upon photodetachment of an electron to produce either the singlet or triplet states, with greater activity of this mode in the triplet state. In addition, significant excitation of the torsional mode is expected in the triplet state. As discussed above, both low-lying states observed in the spectra do display considerable activity due to the symmetric scissors mode. This activity is somewhat more pronounced in the ã state, providing further support for the assignment of this state as the triplet. The calculated harmonic frequencies for this mode in both the singlet and triplet states and their shifts upon deuteriation are in good agreement with experiment. As an example, for TME $^3B_1$, the (unscaled) B3LYP harmonic frequencies are $\omega_{\text{scissors}} = 366\ \text{cm}^{-1}$ and $312\ \text{cm}^{-1}$ for the C_6H_8 and C_6D_8 isotopomers, respectively. From Fig. 2, the corresponding experimental values are 335 and 267 cm^{-1} for the ã state (here assigned to the triplet). However, while experiment gives the same value of the CCC stretch frequency in the two states (to within experimental resolution), the TCSCF/ROHF calculations predict a 38 cm^{-1} lower value of the frequency in the singlet state. This could reflect an inadequacy of the TCSCF/ROHF procedure for calculating the frequencies.

The lack of visible structure due to the twisting mode can be understood in terms of its low value (ω_{torsion} is calculated to be 86 cm^{-1} for the $^3B_1$ state and 32 cm^{-1} in the singlet state). As a result, it is not expected to be resolved in the spectrum. Given the large difference in the equilibrium values of the dihedral angle between the two allyl groups in the $^3B_1$ neutral and $^2B_1$ anionic species, there arises the question as to whether the origin in the twisting mode is observed in the photoelectron spectrum. The relevant potential energy curves, calculated at the B3LYP level, are shown in Figs. 6 and 7. The B3LYP calculations like earlier CI results[27] predict a torsional barrier in TME ã $^3B_1$ of roughly 1 kcal mol^{-1}. From Fig. 7 it is seen that only the levels near the top of the torsional barrier in the $^3B_1$ state are likely to be accessible upon photodetachment of an electron from the anion.

The photoelectron spectra of [TME]$^-$ in Figs. 2 and 3 show no evidence of torsional excitation. It is very difficult for our spectrometer to resolve vibrational modes with frequencies less than 100 cm^{-1}, particularly if the Franck–Condon factors are poor. However, several electronic structure calculations with methods as different as DFT/B3LYP, MCSCF, and MP2 all predict ^{3}[TME] to have a D_2 equilibrium geometry with a twist angle of about 50° and a torsional frequency of roughly 80 cm^{-1}. Consequently we cannot be certain if the TME ã origin that we observe is truly the (0,0) feature.

In the light of these considerations, we conclude that the 3.0 ± 0.3 kcal mol^{-1} singlet–triplet separation deduced from the photoelectron spectrum in Fig. 2 probably overestimates the singlet–triplet gap by approximately the energy difference between the triplet at its D_2 minimum and at its D_{2d} saddle-point structure. This difference is calculated to be 1 kcal mol^{-1} with both the present B3LYP and the earlier MCSCF/CI calculations. Thus we conclude that the singlet–triplet splitting in TME is actually about 2 kcal mol^{-1}, with the singlet being more stable. A more detailed analysis of the ^{3}TME ã $\longleftarrow$ [TME]$^-$ origin and the torsional Franck–Condon factors will be reported later.

Based on gas-phase negative ion photoelectron spectra, our conclusion is that the ground state of the isolated $[(CH_2)_2C{-}C(CH_2)_2]$ diradical is the singlet, $\tilde{X}$ ^1A. We find ^{1}TME to be approximately 2 kcal mol^{-1} more stable than ^{3}TME. These *gas phase* results appear to be inconsistent with earlier *matrix isolation* studies. Isolation of the TME diradical in a matrix clearly permits EPR detection of the triplet hydrocarbon. Irradiation of 2,3-dimethylenecyclopentanone in liquid N_2 generated[1]

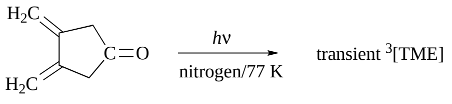

(12a)

transient EPR signals from ^{3}TME, eqn. (12a). In contrast, irradiation of the diazo precursor in a different matrix (methyltetrahydrofuran or methylcyclohexane glass) at a lower temperature produced[9] intense ^{3}[TME] signals that persisted indefinitely.

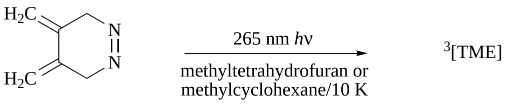

(12b)

One possible 'solution' to this dilemma is that ^{3}TME in its equilibrium structure isolated in the methyltetrahydrofuran glass lies energetically *below* ^{1}TME (at the triplet geometry). For the TME diradical the torsional coordinate (τ) is likely to be the key to ^{3}[TME] $\rightleftharpoons$ ^{1}[TME] interconversion. If the methyltetrahydrofuran 'solvent' molecules lock the triplet into the twisted structure, the interconversion could be drastically slowed down. In this case ^{3}TME would be 'metastable.' That is to say, if ^{3}TME were formed in its ground rotational/vibrational state, it would decay only slowly back to the ground ^{1}TME. The spin–orbit matrix elements that couple the ã $^3B_1$ and $\tilde{X}$ ^1A states of TME have not been measured but there is active theoretical work directed to this end.[55]

CI calculations[27] indicated that for the gas phase molecule and at the triplet geometry, the triplet lies about 1.5 kcal mol^{-1} below the singlet, but the results of the present study suggest that at the D_{2d} structure there was a bias of roughly 2 kcal mol^{-1} toward the triplet state in these CI calculations. One of the approximations in these calculations was the use of CASSCF(6,6)/3–21G geometries. Whether this could introduce a larger error for $\tau = 90°$ than for $\tau \cong 50°$ is not known. Given the small energy differences involved (2 kcal mol$^{-1} \cong 700$ cm^{-1}), it is not possible, based on available information, to decide whether matrix-isolated TME does display triplet metastability.

Finally, we compare the thermochemistry of TME with that of other radicals. Because the 2-(isopropenyl)allyl radial and the TME diradical are both 'allylic', it is interesting to contrast the energetics of these species with allyl radical itself.[56] The bond energy of propene is measured to be D_0-(CH_2CHCH_2–H) = 87.4 ± 0.4 kcal mol^{-1}. We find that 2,3-dimethylbuta-1,3-diene has a 'normal' allylic C–H bond, D_0-[CH_2=C(CH_3)C(CH_2)CH_2–H] = 88 ± 3 kcal mol^{-1}, while the 2-(isopropenyl)allyl radical has D_0[(CH_2)$_2$CC(CH_2)CH_2–H] = 93 ± 4 kcal mol^{-1}.

Acknowledgements

We are privileged to acknowledge that this collaboration pursuing the TME diradical is a direct result from the intellectual leadership provided by Paul Dowd. Paul's interest in defining the chemical properties of TME and his wide appreciation of all areas of chemistry were instrumental in seeing that the initial suggestion for the project culminated in this report. In addition to encouraging our efforts, Paul actively participated in this project, initially in defining the synthesis of the gas-phase ionic precursor to TME, and, for this report, in allowing his postdoctoral fellow (C. X. W.) to prepare the deuteriated ion precursor reported above.[3] We wish to dedicate this paper, a report that completes the circle of one aspect of his scientific work, to the memory of Paul Dowd, a person whom we will always remember as a scholar, a scientist, a teacher, and a friend.

G. B. E. is supported by a grant from the Chemical Physics Program, United States Department of Energy (DE-FG02–87ER13695). We also thank the National Science Foundation for support through grants CHE97–03486 and PHY95–12150 to W. C. L., CHE94–07080 (J. J. G.) and CHE94–22210 (K. D. J.). K. D. J. is pleased to acknowledge JILA for a Visiting Fellowship. We thank Jiang Zhao for help with the acidity measurements and Profs. J. A. Berson and C. H. Greene for helpful discussions.

References

1 P. Dowd, *J. Am. Chem. Soc.*, 1970, **92**, 1066.
2 J. A. Berson, *Acc. Chem. Res.*, 1997, **30**, 238.
3 J. Lee, P. K. Chou, P. Dowd and J. J. Grabowski, *J. Am. Chem. Soc.*, 1993, **115**, 7902.
4 W. T. Borden, 'Effects of Electron Repulsion in Diradicals', in *Diradicals*, ed. W. T. Borden, Wiley, New York, 1982.
5 M. Bersohn and J. C. Baird, *An Introduction to Electron Paramagnetic Resonance*, Benjamin, 1966. On p. 76, it is claimed: 'At this writing, the smallest sample that the best spectrometer can see is about 10(–14) moles of unpaired electrons per gauss of line width.' With current technologies, it is likely that one can improve on this by an order-of-magnitude.
6 W. Weltner Jr., *Magnetic Atoms and Molecules*, Van Nostrand Reinhold, New York, 1983.
7 W. R. Roth and G. Erker, *Angew. Chem., Int. Ed. Engl.*, 1973, **12**, 503.
8 W. R. Roth, M. Biermann, G. Erker, K. Jelich, W. Gerhartz and H. Gorner, *Chem. Ber.*, 1980, **113**, 586.
9 P. Dowd, W. Chang and Y. H. Paik, *J. Am. Chem. Soc.*, 1986, **108**, 7416.
10 K. J. Stone, M. M. Greenberg, J. L. Goodman, K. S. Peters and J. A. Berson, *J. Am. Chem. Soc.*, 1986, **108**, 8088.
11 W. R. Roth, U. Kowalczik, G. Maier, P. R. Reisenauer and W. Muller, *Angew. Chem., Int. Ed. Engl.*, 1987, **26**, 1285.
12 P. Dowd, W. Chang and Y. H. Paik, *J. Am. Chem. Soc.*, 1987, **109**, 5284.
13 P. G. Wenthold, J. Ju and R. R. Squires, *J. Am. Chem. Soc.*, 1994, **116**, 6961.
14 P. G. Wenthold and R. R. Squires, *J. Am. Chem. Soc.*, 1994, **116**, 6401.
15 D. G. Leopold, K. K. Murray, A. E. Stevens-Miller and W. C. Lineberger, *J. Chem. Phys.*, 1985, **83**, 4849.
16 D. G. Leopold, A. E. Stevens Miller and W. C. Lineberger, *J. Am. Chem. Soc.*, 1986, **108**, 1379.
17 S. Pedersen, J. L. Herek and A. H. Zewail, *Science*, 1994, **266**, 1359.
18 J. A. Berson, *Science*, 1994, **266**, 1338.
19 C. Doubleday Jr., K. Bolton, G. H. Peslherbe and W. L. Hase, *J. Am. Chem. Soc.*, 1996, **118**, 9922.
20 B. K. Carpenter, *Am. Scientist*, 1997, **85**, 138.
21 P. Du and W. T. Borden, *J. Am. Chem. Soc.*, 1987, **109**, 930.
22 P. Du and W. T. Borden, *J. Am. Chem. Soc.*, 1992, **114**, 4949.
23 W. T. Borden, H. Iwamura and J. A. Berson, *Acc. Chem. Res.*, 1994, **27**, 109.
24 Y. Choi, K. D. Jordan, Y. H. Paik, W. Chang and P. Dowd, *J. Am. Chem. Soc.*, 1988, **110**, 7575.
25 P. Nachtigall, P. Dowd and K. D. Jordan, *J. Am. Chem. Soc.*, 1992, **114**, 4747.
26 P. Nachtigall and K. D. Jordan, *J. Am. Chem. Soc.*, 1992, **114**, 4743.
27 P. Nachtigall and K. D. Jordan, *J. Am. Chem. Soc.*, 1993, **115**, 270.
28 J. J. Nash, P. Dowd and K. D. Jordan, *J. Am. Chem. Soc.*, 1992, **114**, 10 071.
29 K. Matsuda and H. Iwamura, *J. Am. Chem. Soc.*, 1997, **119**, 7412.
30 J. Lee and J. J. Grabowski, *Chem. Rev.*, 1992, **92**, 1611.
31 K. M. Ervin and W. C. Lineberger, 'Negative Ion Photoelectron Spectroscopy', in *Advances in Gas Phase Ion Chemistry*, eds. N. G. Adams and L. M. Babcock, JAI Press, Greenwich, CT, 1992.
32 D. M. Neumark, K. R. Lykke, T. Andersen and W. C. Lineberger, *Phys. Rev. A*, 1985, **32**, 1890. E_{ea}(O) = 11 784.645 ± 0.006 cm^{-1} or 1.461 110 ± 0.000 001 eV.
33 M. W. Siegel, R. J. Celotta, J. L. Hall, J. Levine and R. A. Bennett, *Phys. Rev. A*, 1972, **6**, 607.
34 J. J. Grabowski and S. J. Melly, *Int. J. Mass Spectrom. Ion Proc.*, 1987, **81**, 147.
35 S. T. Graul and R. R. Squires, *Mass Spectrom. Rev.*, 1988, **7**, 263.
36 J. J. Grabowski, 'Flowing Afterglow Studies of Carbene Anions', in *Advances in Gas Phase Ion Chemistry*, eds. L. M. Babcock and N. Adams, JAI Press, Greenwich, CT, 1992.
37 S. G. Lias, J. E. Bartmess, J. F. Liebman, J. L. Holmes, R. D. Levin and W. G. Mallard, *J. Phys. Chem. Ref. Data*, 1988, **17** (supplement 1), 1. Most of the acidities are taken from the NIST Negative Ion Energetics Database, Version 3.00, NIST Standard Reference Database 19B, October 1993. NEGION.
38 S. E. Barlow, T. T. Dang and V. M. Bierbaum, *J. Am. Chem. Soc.*, 1990, **112**, 6832.
39 M. S. Robinson, M. L. Polak, V. M. Bierbaum, C. H. DePuy and W. C. Lineberger, *J. Am. Chem. Soc.*, 1995, **117**, 6766.
40 J. J. Grabowski and D. Owusu, 1997, unpublished work. $\Delta_{acid}G_{298}$(furan) = 382.9 ± 0.2 kcal mol^{-1} and $\Delta_{acid}H_{298}$(furan) = 390.7 ± 0.2 kcal mol^{-1}.
41 G. E. Davico, V. M. Bierbaum, C. H. DePuy, G. B. Ellison and R. R. Squires, *J. Am. Chem. Soc.*, 1995, **117**, 2590. The entropy for ionization, $AH \longrightarrow A^- + H^+$ can be approximated by expression (A9): $\Delta_{acid}S_T \cong 3/2\ R\ \ln|M(A^-)/M(AH)| + R/2\ \ln\ |A_0B_0C_0(AH)/A_0B_0C_0(A^-)| + R\ln|\sigma(AH)/\sigma(A^-)| + S_T(H^+)$.
42 P. G. Wenthold, M. L. Polak and W. C. Lineberger, *J. Phys. Chem.*, 1996, **100**, 6920.
43 J. Berkowitz, G. B. Ellison and D. Gutman, *J. Phys. Chem.*, 1994, **98**, 2744.
44 C. R. Moylan and J. I. Brauman, *Ann. Rev. Phys. Chem.*, 1983, **34**, 187.
45 J. B. Pedley, R. D. Naylor and S. P. Kirby, *Thermochemical Data of Organic Compounds*, Chapman and Hall, 1986.
46 F. K. Meyer, J. M. Jasinski, R. N. Rosenfeld and J. I. Brauman, *J. Am. Chem. Soc.*, 1982, **104**, 663.
47 J. M. Oakes and G. B. Ellison, *J. Am. Chem. Soc.*, 1984, **106**, 7734.
48 C. H. Greene, G. B. Ellison and K. D. Jordan, 1997, unpublished results.
49 P. G. Wenthold, J. Hu, R. R. Squires and W. C. Lineberger, *J. Am. Chem. Soc.*, 1996, **118**, 475.
50 E. P. Clifford, P. G. Wenthold, W. C. Lineberger, G. A. Petersson, K. A. Broadus, S. R. Kass, S. Kato, C. H. DePuy, V. M. Bierbaum and G. B. Ellison, *J. Phys. Chem.*, submitted, Sept. 1997.

51 The B3LYP functional combines Becke's hybrid exchange functional (A. D. Becke, *J. Chem. Phys.*, 1993, **98**, 5648) and the LYP correlation functional [C. Lee, W. Yang and R. G. Parr, *Phys. Rev. B*, 1988, **37**, 785) with the weights of the various terms in the functional being the default values in GAUSSIAN 94.
52 T. Clark, J. Chandrasekhar, G. W. Spitznagel and P. v. R. Schleyer, *J. Comput. Chem.*, 1983, **4**, 294.
53 W. J. Hehre, R. Ditchfield and J. A. Pople, *J. Chem. Phys.*, 1972, **56**, 2257.
54 M. J. Frisch, G. W. Trucks, H. B. Schlegel, P. M. W. Gill, B. G. Johnson, M. A. Robb, J. R. Cheeseman, T. Keith, G. A. Petersson, J. A. Montgomery, K. Raghavachari, M. A. Al-Laham, V. G. Zakrzewski, J. V. Ortiz, J. B. Foresman, J. Cioslowski, B. B. Stefanov, A. Nanayakkara, M. Challacombe, C. Y. Peng, P. Y. Ayala, W. Chen, M. W. Wong, J. L. Andres, E. S. Replogle, R. Gomperts, R. L. Martin, D. J. Fox, J. S. Binkley, D. J. Defrees, J. Baker, J. P. Stewart, M. Head-Gordon, C. Gonzalez and J. A. Pople, GAUSSIAN 94, Revision C.2, Gaussian, Inc., Pittsburgh, PA, 1996.
55 J. Michl, *J. Am. Chem. Soc.*, 1996, **118**, 3568.
56 G. B. Ellison, G. E. Davico, V. M. Bierbaum and C. H. DePuy, *Int. J. Mass Spectrom. Ion Proc.*, 1996, **156**, 109.

Paper 7/07322D
Received 9*th October* 1997
Accepted 27*th November* 1997